

Finite Element Stress Analysis and Multi-parameter Optimization of a High-pressure Vessel

Alexey I. Borovkov

Dmitriy S. Mikhaleuk

Computational Mechanics Laboratory, St.Petersburg State Technical University,
Russia

Abstract

This paper describes the results of 3D structural contact FE analysis of high-pressure vessel (HPV). The research is carried out to analyze stress concentration zones and to determine variables for design optimization. The submodeling method is used to analyze zones with complex geometry. Experimental strain measurements are used to verify the 3D model and the obtained results. The comparison of experimental results and FE modeling is presented. The description of methods and results of multi-parameter design optimization are presented. Such important results of optimization as the decrease of steel intensity and outline size of the HPV are obtained.

The multiplier of HPV is used for the external pressure increase and transfer to the working sell. Various material models are used to describe multiplier parts. The results of multiplier 3D structural contact analysis are presented.

The importance of the results obtained and good correlation with experiments make it possible to carry out similar analyses for various HPV that are widely used in industry.

Introduction

Diamond is natural substance, precious stone, and industrial stock. About 80% of all extracted diamonds are related to industrial ones, used for producing diamond tools. The most important fields of industrial application of diamonds and tools manufactured from them are the following:

- 1) machining hard-alloy parts of mechanisms and machines;
- 2) boring geological rifts in hard rocks;
- 3) cutting parts of high-hardness and high-temperature materials;
- 4) grinding and polishing super-hard coating materials.

Since Antoine Lavoisier in 1792 and Smithson Tenet in 1797 demonstrated that diamond and graphite were only different forms of the same substance – carbon, multiple endeavors have been undertaken for transformation of graphite, relatively often met in nature, into rare and valuable diamond. However, only during 1950-60 decade people managed to obtain artificial diamonds, about 0.1 mm in diameter.

Proceeding from differences between diamond and graphite at atomic level, it has been shown that graphite may be transformed into diamond by applying super-high external pressure sufficient for changing atom positions in lattice. At present, for manufacturing of artificial diamonds from graphite (artificial diamonds synthesis), high-pressure vessels (HPV) making it possible to raise pressure in the operating space up to 100,000 atm are used [4].

This paper describes the finite element modeling (FEM) and the structural analysis as well as design optimization of HPV used for artificial diamond synthesis. The general view of the vessel is shown in Figure 1 - *Overall view of vessel*. Vessel operating is based on external pressure transferring to an operating cell with the use of a multi-punch double-stage multiplier located inside the vessel body. Under pressure P oil enters through an inlet conduit into the free space between internal spherical surfaces of half-case bodies and the outer spherical surface of a membrane made of incompressible polymer. The membrane is designated for oil pressure transferring onto the outer surface of the steel punches. Eight punches in assembly present a cut sphere with octahedron shape inside (See Figure 2 - *Cut sphere*). Between adjacent

surfaces of adjoining punches, leveling gaskets are disposed for providing uniform movement of punches to the center under applied external pressure (See Figure 3 - *Leveling gaskets*). To prevent the membrane from the "flowing-in" and getting into the space between punches, steel plates are placed on the outer surface of the cut sphere (See Figure 4 - *Steel plates*). Punches transfer pressure onto 6 hard-alloy inserts shown in Figure 5 - *Hard-alloy inserts*. During artificial diamonds synthesizing, it's necessary to provide the oil-tightness of the operating sell. With this aim locking gaskets shown in Figure 6 - *Locking gaskets* are placed between adjacent surfaces of hard-alloy inserts. The inner surface of hard-alloy inserts in assembly makes a cubic operating area (See Figure 7 - *Operating area*). A metallic capsule of the cubic shape is installed in the operating area. Inside this area there is a cylindrical hollow where graphite intended for being transformed into diamond is placed.

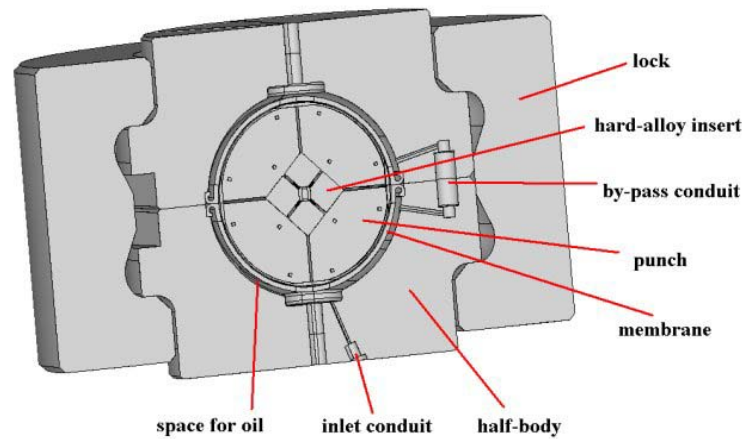


Figure 1 - Overall view of vessel

ANSYS

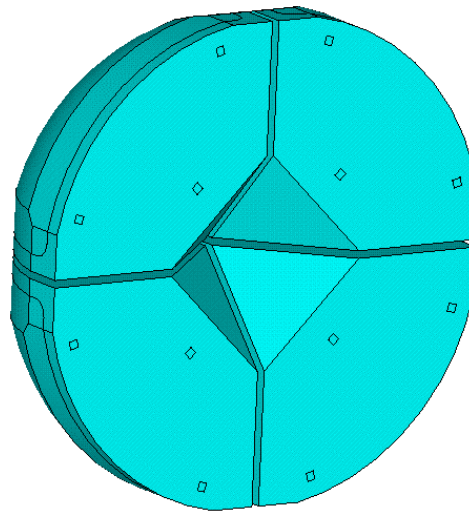


Figure 2 - Cut sphere

ANSYS

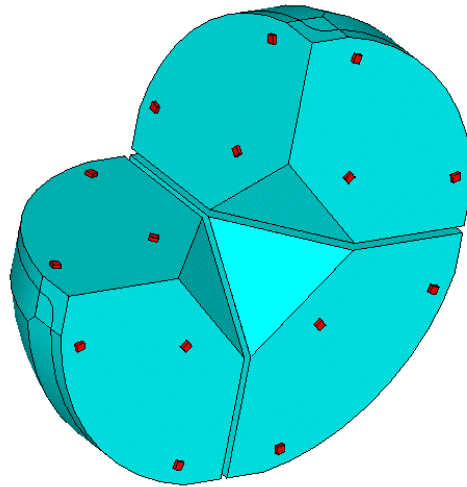


Figure 3 - Leveling gaskets

ANSYS

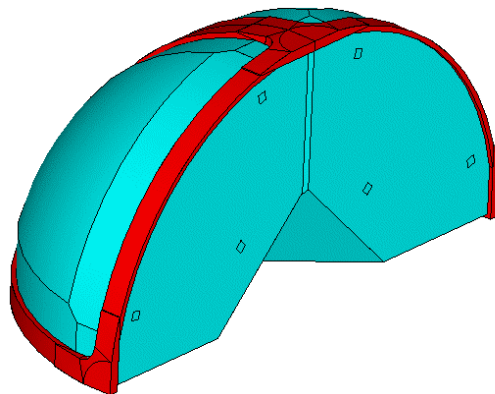


Figure 4 - Steel plates

ANSYS

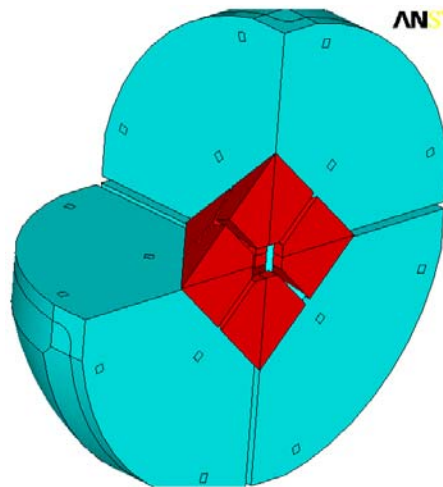


Figure 5 - Hard-alloy inserts

ANSYS

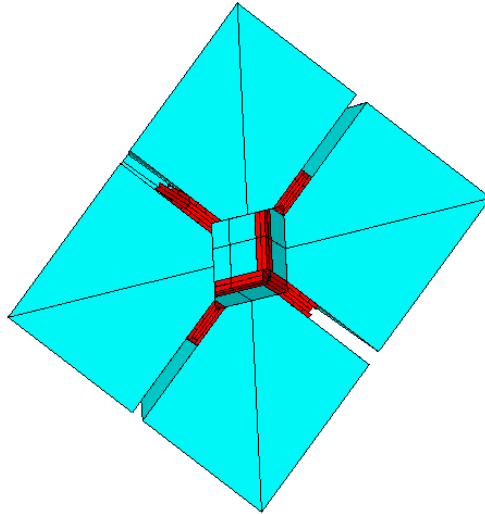


Figure 6 - Locking gaskets

ANSYS

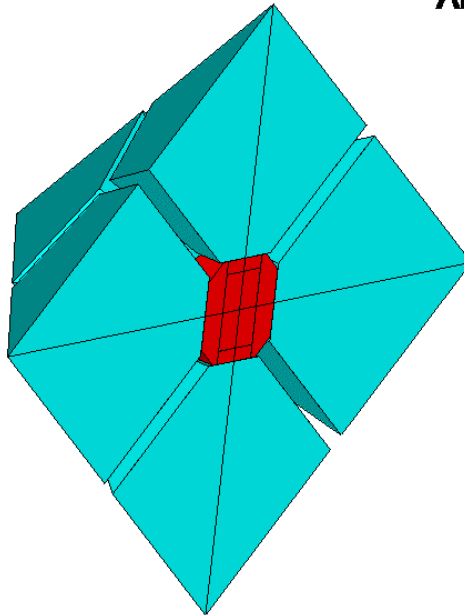


Figure 7 - Operating area

Proceeding from the fact that in the production process there is no mechanical interaction between case body parts and the membrane, the procedure of the structural analysis of the vessel can be divided into two independent stages: analysis of the case body parts and that for multiplier components.

Case Body Structural Analysis

FE Model and Analysis Procedure

The main components of the vessel are case body parts: upper and lower half-bodies and locks. A general view of case body parts is presented in Figure 8 - *Case body*: two half-circles of the lock with outer radius R_1 , upper and lower half-bodies with exterior radius R_2 . The inner surface of the half-bodies in assembly presents a sphere with radius R_3 . The vessel is loaded by internal pressure P , uniformly distributed throughout inner hemispherical surfaces of the half-bodies. Owing to the loads applied, the upper and the lower half-bodies tend to separate, what is hampered by the lock half-circles. Owing to the symmetry of construction and boundary conditions, we may analyze only a half of body parts.

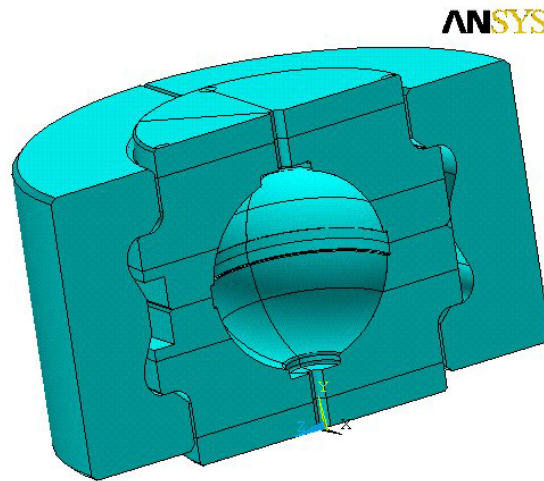


Figure 8 - Case body

Within the ANSYS software a 3D model of a half of the case body parts including the upper and the lower half-bodies as well as the lock half-circles was developed. The 3D FE model contains 42740 SOLID45 elements (See Figure 9 - *FE model of Case body*). Possibility of reciprocal sliding of locks and half-bodies in the contact interaction area is taken into account. For description of contact interaction the Coulomb's law was selected. Coefficient of friction was assumed to be equal to 0.2. Contact interaction was simulated in ANSYS with the use of CONTA172 and TARGE169 elements.

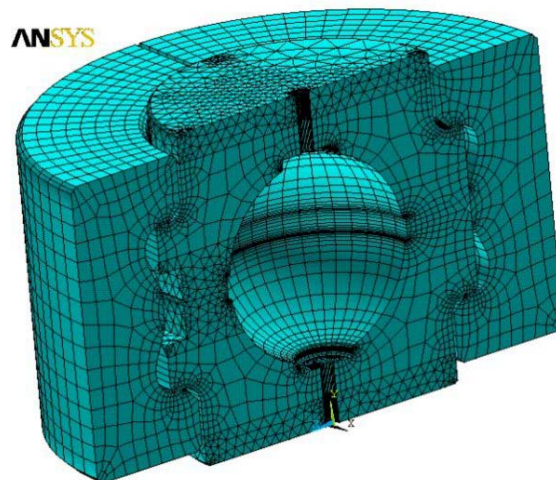


Figure 9 - FE model of case body

Equivalent stress distribution in the lock is presented in Figure 10 - *Equivalent stress in the Lock*, from which it follows that equivalent stress in the zone of curvature, what is stress concentrator, is distributed irregularly and depends on position of vertical cross section. Maximal stresses in the construction originate in the half-body - lock contact area (see Figure 11 - *Stress concentrator*).

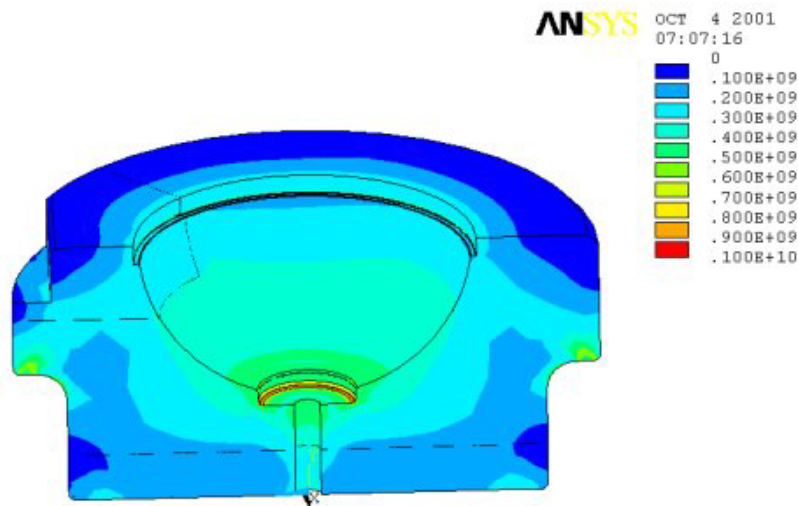


Figure 10 - Equivalent stress in the lock

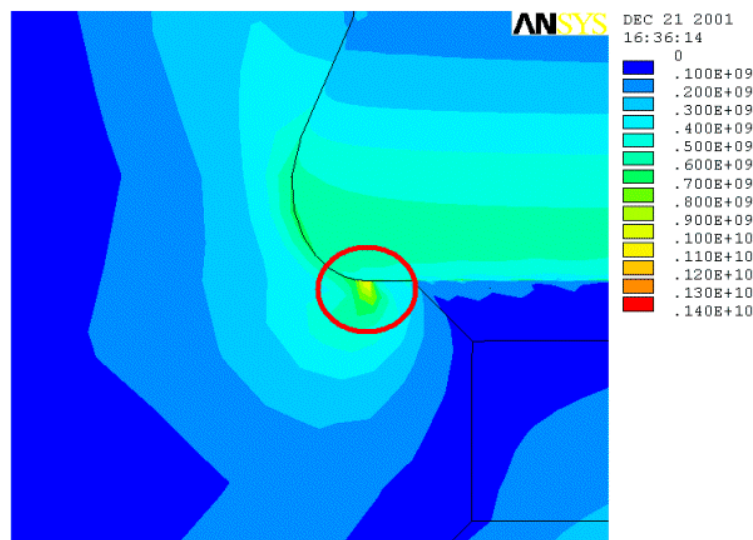


Figure 11 - Stress concentrator

Equivalent stress distribution in the lower half body is presented in Figure 12 - *Equivalent stress in the half body1*. The main areas of stress concentration are the curvatures on the outer and inner surfaces (see Figure 13 - *Equivalent stress in the half body 2*).

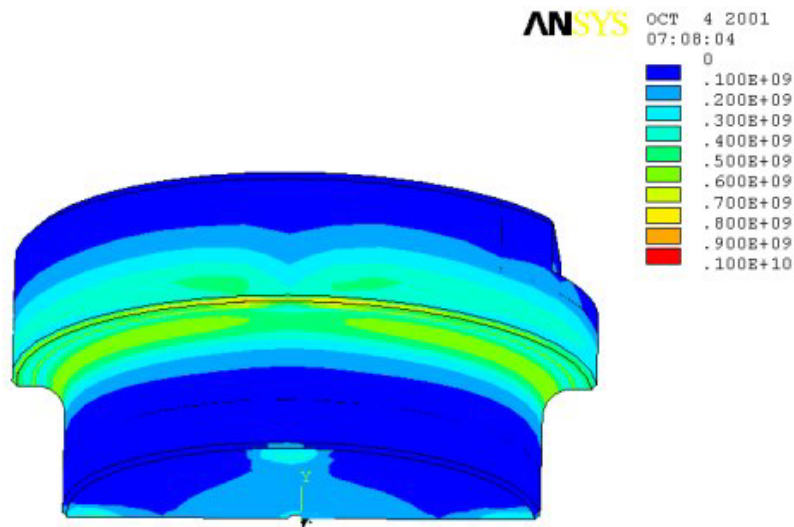


Figure 12 - Equivalent stress in the half body 1

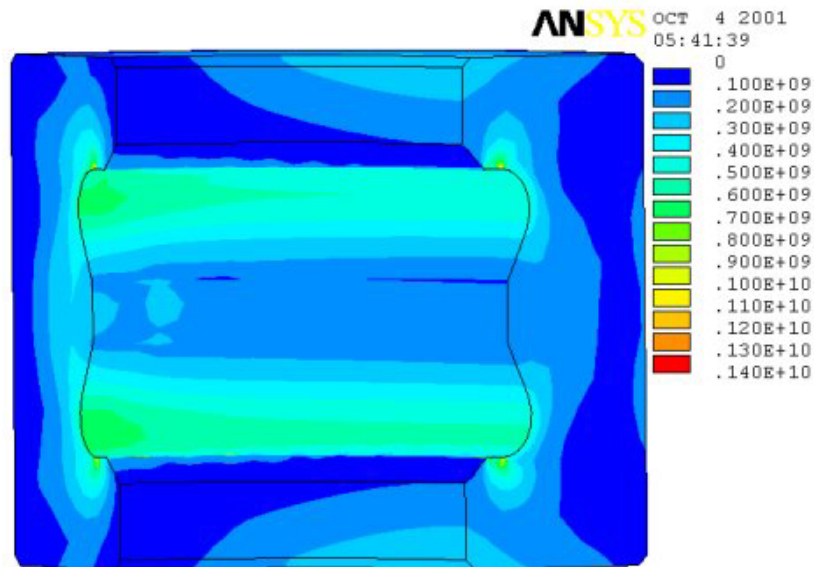


Figure 13 - Equivalent stress in the half body 2

Submodeling

For analysis of the local 3D stressed state in the vicinity of the inlet and by-pass conduits, a separate investigation was carried out. For effective solution of this problem and obtaining FE results with the high degree of accuracy, the submodeling method was applied. Figure 14 - *Upper submodel* demonstrates the 3D model of the half-body fragment containing the upper by-pass conduit. The FE model contains 53104 SOLID92 elements.

As the result of solution of 3D linear elastic problem, there was obtained equivalent stress distribution for the investigated fragment, presented in Figure 15 - *Equivalent stress in the upper submodel 1*. Analyzing the defined equivalent stress field, one may notice the presence of a single stress concentrator (Figure - 16 *Equivalent stress in the upper submodel 2*). Equivalent stress level in this area exceeds tensile strength for the material. The cause of stress concentration appearance is short-distance location of the conduit outlet to the operating area of a by-pass valve.

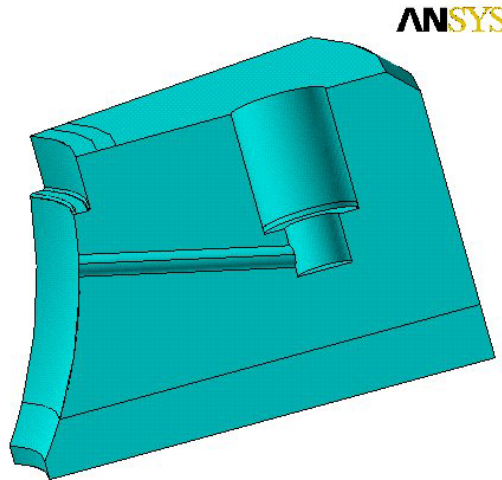


Figure 14 - Upper submodel

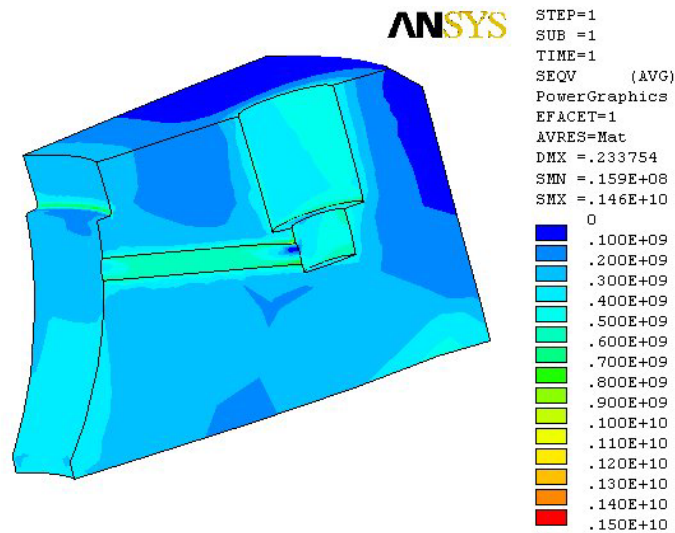


Figure 15 - Equivalent stress in the upper submodel 1

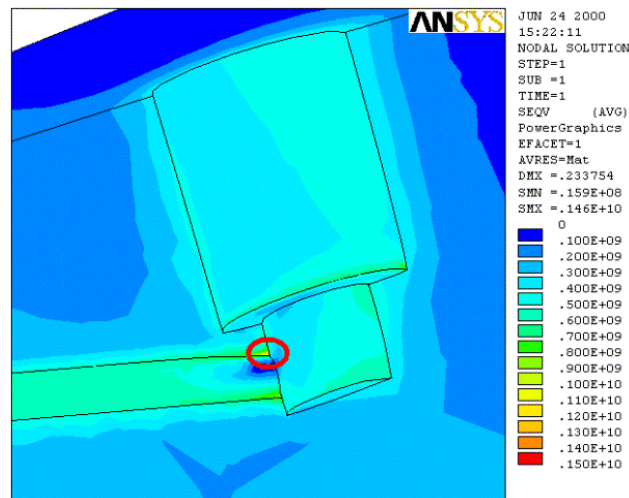


Figure 16 - Equivalent stress in the upper submodel 2

Besides, in the lower part of the half-body there are one inlet and four other technological conduits, which are not subjected to internal pressure. 3D structural analysis of the lower part of the half-body was performed with account of both the technological conduits and the lower inlet conduit. The 3D FE model of the lower part of the half-body, containing 97395 SOLID92 elements and 453267 degrees of freedom, is presented in Figure 17 - *FE model of the lower submodel*.

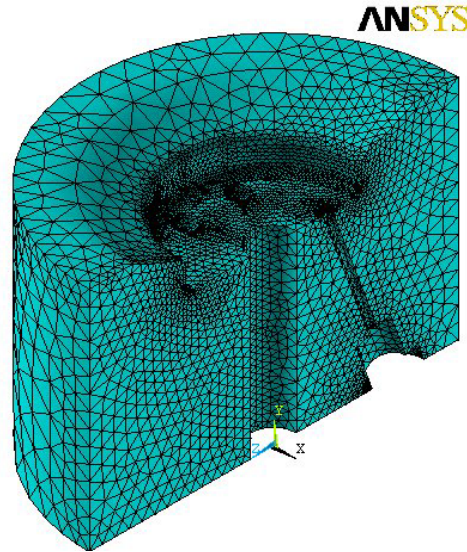


Figure 17 - FE model of the lower submodel

The equivalent stress distribution is shown in Figure 18 - *Equivalent stress in the lower submodel 1*. Figure 19 - *Equivalent stress in the lower submodel 2* demonstrates a model fragment. The cross-section is presented for visualization of the stress distribution inside the unloaded technological conduit. Analyzing the results obtained one can notice that unloaded conduits do not represent additional stress concentration. Besides, they decrease stress level in local areas of their influence.

Characteristic element size for the stress concentration zones in all problems was estimated based on convergence analysis.

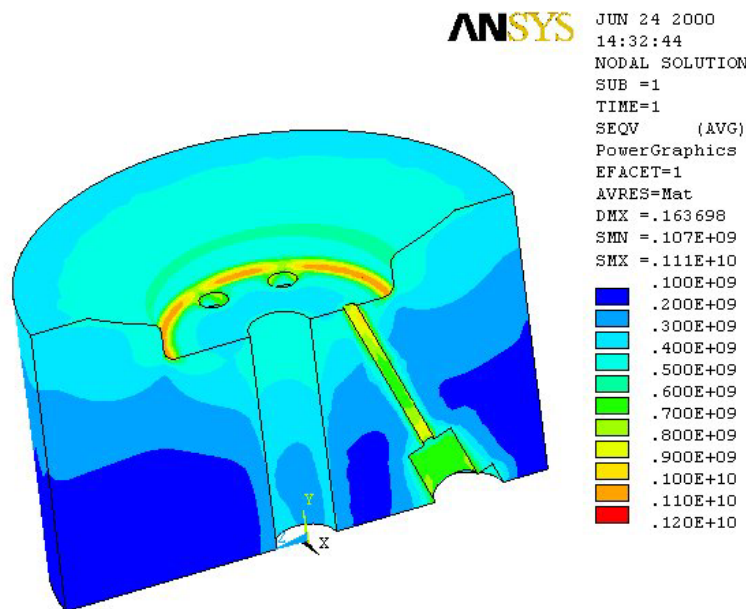


Figure 18 - Equivalent stress in the lower submodel 1

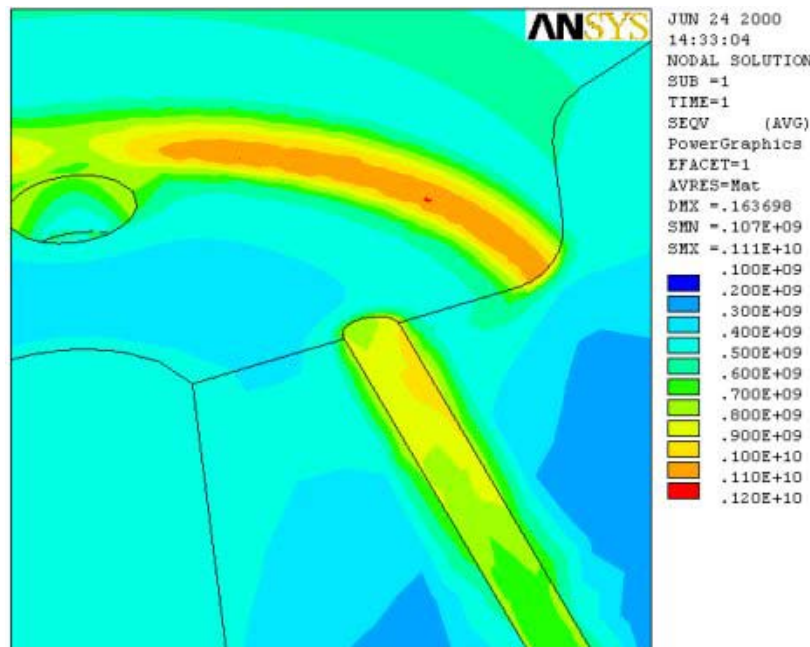


Figure 19 - Equivalent stress in the lower submodel 2

Experimental Research

Experiment Description

For substantiation of selected numerical methods and confirmation of the mathematical models taken as a basis in FE structural analysis of the vessel case body parts, there was carried out an experimental research of strain fields using the strain-measuring method [6].

For measurement implementation, there were used strain sensors with film support and a digital strain-measuring tensometric bridge with automatic balancing. Compensating strain gages were glued onto a separate plate, not subjected to deformation. Strain gages disposition (see Figure 20 - *Sensors positions*) was based on FEA results. It was showed previously that maximal stresses in the construction originate in the half-body - lock contact area, but this area can't be experimentally analyzed with use of strain-measuring method. Except from contact surface there is one stress concentration zone of interest - the curvature area on the inner surface of the lock. This fact determined 6 spots for strain gages disposition. Two strain gages are used for measuring correspondingly ε_z and ε_ϕ . For strain determination on the lateral surface of the lock, one more pair of strain-gages measuring was ε_z and ε_r used.

The vessel loading was implemented by operation pressure, increasing from 0 to 1500 atm with 500 atm - steps and unloading down to 500 atm. Readings were taken correspondingly at the operation pressure values of 500, 1000, 1500, 1000 and 500 atm.

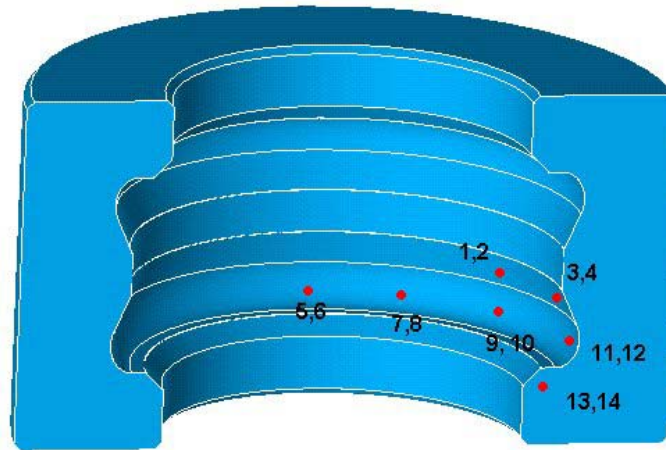


Figure 20 - Sensors positions

Results

To compare results of FE simulation and those of experimental research, the quasi-static non-linear problem of case body loading and unloading was solved. Five load steps corresponded to five operation pressure values at which the readings were taken during the experiment.

The results of comparing strains values obtained by FE analysis and by experiment for three most characteristic areas are presented in Figures 21-23 - *Sensor 1*, *Sensor 2*, and *Sensor 3*. The analysis of the results obtained shows that ANSYS gives the possibility to simulate equivalent stress hysteresis curve. This fact is explained by the existing of contact friction in the model what leads to the non-linearity of the problem. Graphs give evidence of sufficiently good coincidence of the results gotten by the experimental research performed and those obtained by FE analysis: difference does not exceed 10%.

The executed experiment confirms correctness of selected mathematical models for structural analysis of the vessel case body parts.

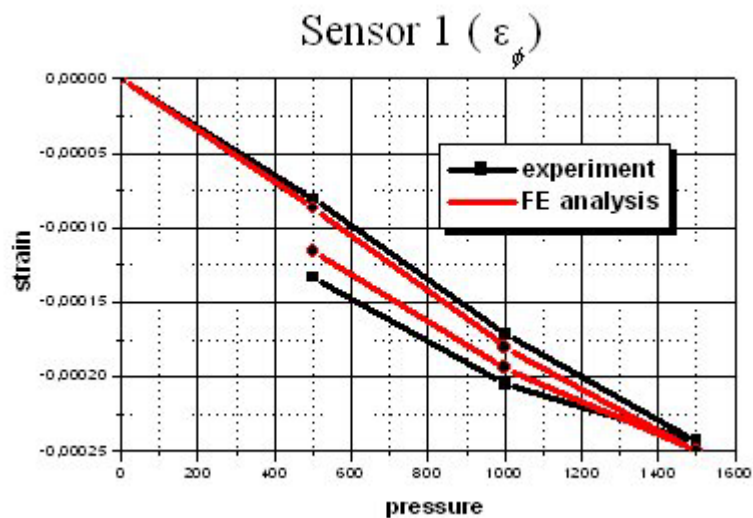


Figure 21 - Sensor 1

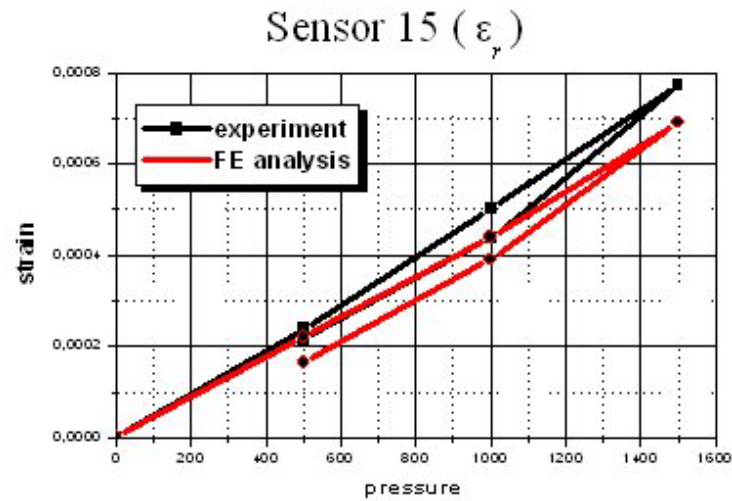


Figure 22 - Sensor 2

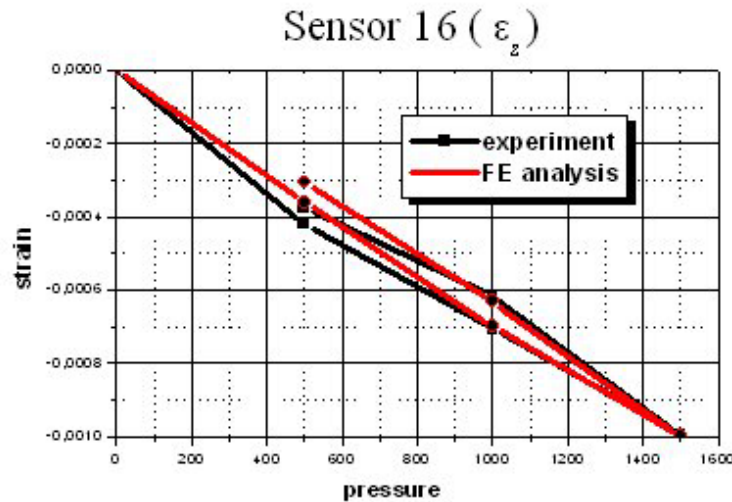


Figure 23 - Sensor 3

Design Optimization

Optimization Criteria and Procedure

Aiming lessening construction mass, the design optimization of size of vessel case body parts was carried out. The optimization problem was solved as axisymmetric for decreasing CPU time.

The independent geometrical parameters R1, R2, H1, H2, H3 marked in Figure 24 - *Design variables* were selected as design variables [2]. Ranges of design variables variation were specified. Maximal equivalent stress values in curvature areas in the half-bodies and in the lock were specified as state variables with the

upper limit. According to the constraints these values are limited by σ_i^* what must provide the necessary safety factor. Total cross-sectional area of the vessel (see Figure 24 - *Design variables*) was selected as objective function to be minimized. It was taken accepted that diminution of cross-sectional area of the vessel case body parts leads to the decrease of volume of the 3D construction and, consequently, to lessening the product mass. The first order method was chosen for optimization implementation.

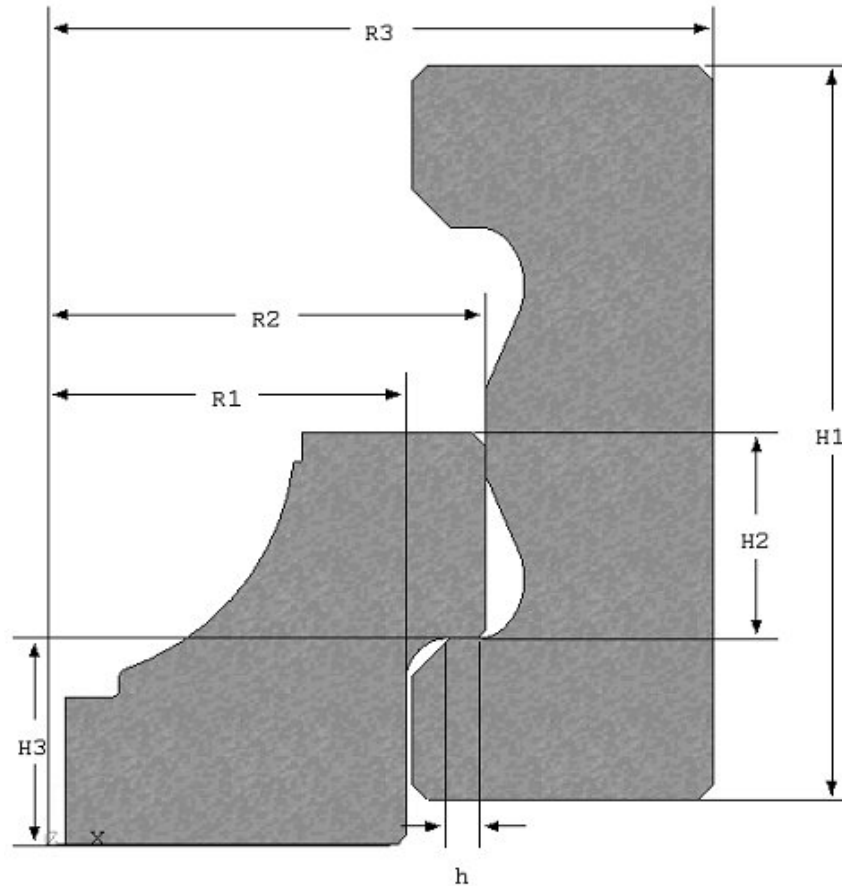


Figure 24 - Design variables

Besides, shape optimization for the curvature on the inner surface of the lock was carried out. A supposition may be made that equivalent stress in the area of curvature depends on its shape, so determination of the optimal shape of the curvature may promote the decrease of equivalent stress value in this area. During the design optimization the shape of the curvature was approximated by a spline passing through points 1,2,3 and 4. X- and Y-coordinates of point 3 were specified as design variables, coordinates of points 1,2 and 4 being kept constant (see Figure 25 - *Curvature*).

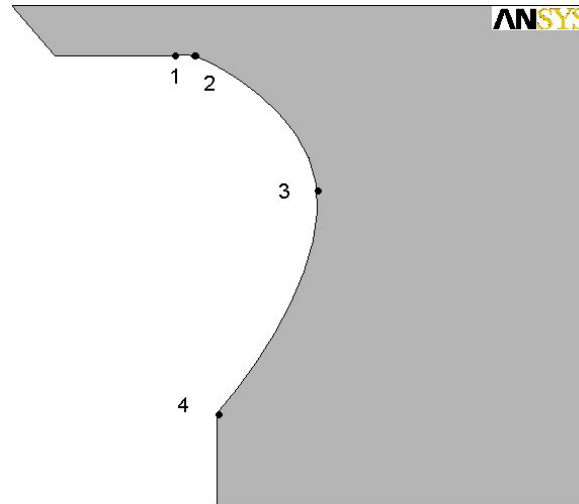


Figure 25 - Curvature

Results

Geometrical models and equivalent stress fields for the original and the optimized designs are presented in Figures 26, 27 - *Initial design*, *Intermediate design*. The optimization performed made it possible to decrease steel intensity of the construction by 27%, maximal outline size - by 13%, therewith lessening maximal equivalent stress by 5%.

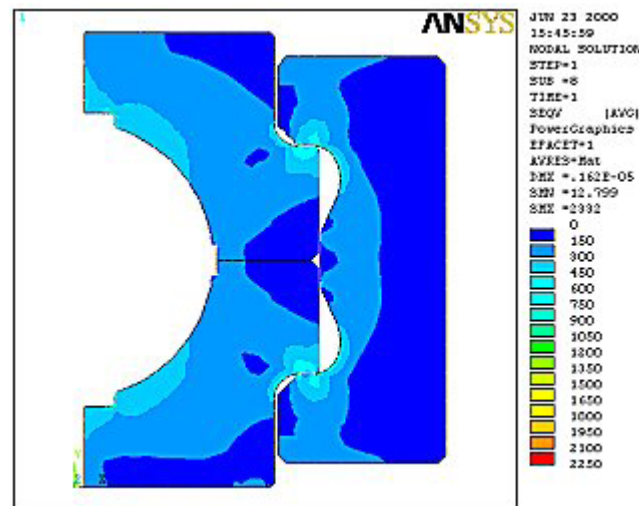


Figure 26 - Initial design

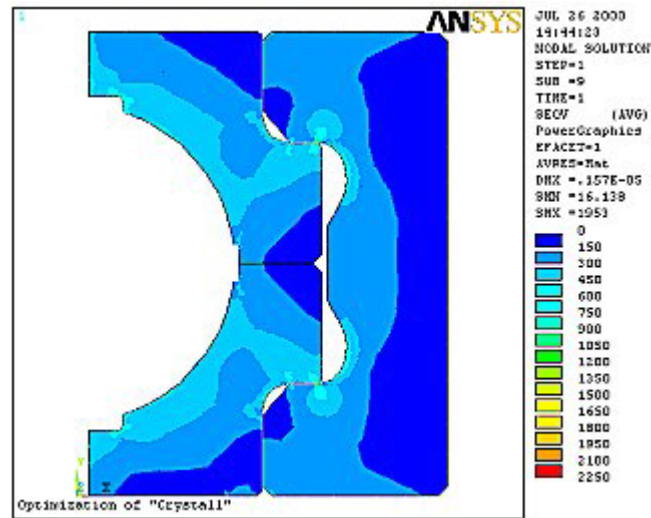


Figure 27 - Intermediate design

Geometrical shape and distribution of equivalent stress in the construction with the optimized shape of the curvature is presented in Figure 28 - *Final design*. It should be marked that in spite of the noticeable change of the curvature shape, it is possible to decrease equivalent stress in the dangerous zone only by 6% compared to that in the original construction.

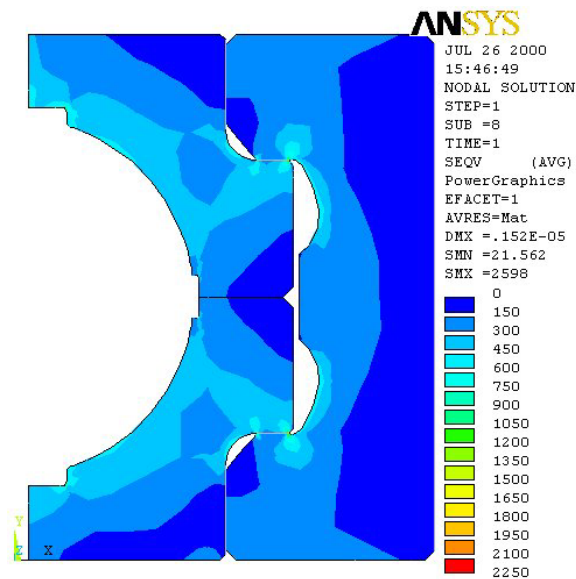


Figure 28 - Final design

Multiplier Structural Analysis

FE model and Analysis Procedure

For evaluation of stressed state of punches and hard-alloy inserts, the structural analysis of multiplier components was carried out. General view of multiplier is presented in Figure 29 - *Multiplier overall view*. For calculations it was assumed that pressure P on the outer surface of a membrane is uniformly transferred to the outer spherical surface of punches. Effect of steel plates is neglected. Owing to the symmetry

of the construction and boundary conditions, only 1/16 part of the multiplier is considered. Possibility of reciprocal slipping between the punch and hard-alloy inserts, between hard-alloy inserts and a metallic capsule is taken into account. Contact interaction was modeled in ANSYS with the use of CONTA172 and TARGE169 elements.

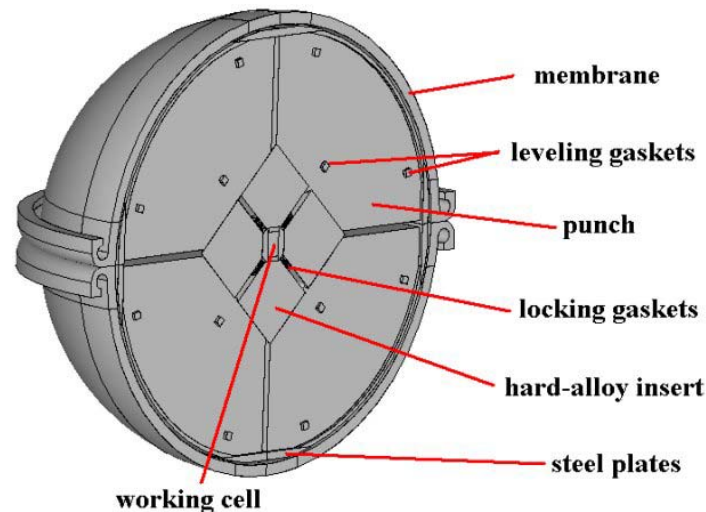


Figure 29 - Multiplier overall view

For 3D stressed state analyzing and obtaining stress distribution throughout a triangular contact area between punches and hard-alloy inserts, multi-layer locking gaskets were virtually replaced by a single-layer anisotropic one for simplification of the problem solution. Effective elastic characteristics were calculated on the basis of Fought and Reiss' relations, presenting a mixture rule for components connected in series and in parallel [3]. Mechanical properties of hard-alloy inserts and the capsule were assumed to be linearly elastic.

The membrane (see Figure 30 - *Membrane*) is made of polymer material. For description of its behavior the Mooney-Rivlin material model was chosen [1,5]. For determination of Mooney-Rivlin constants for membrane material, two types of quasi-static tests of specimens were carried out:

- 1) Uniaxial tension of specimens up to rupture at strain rate 500 mm per minute, ultimate strain being 500-600 %;
- 2) Uniaxial compression of specimens at strain rate 3mm per minute.

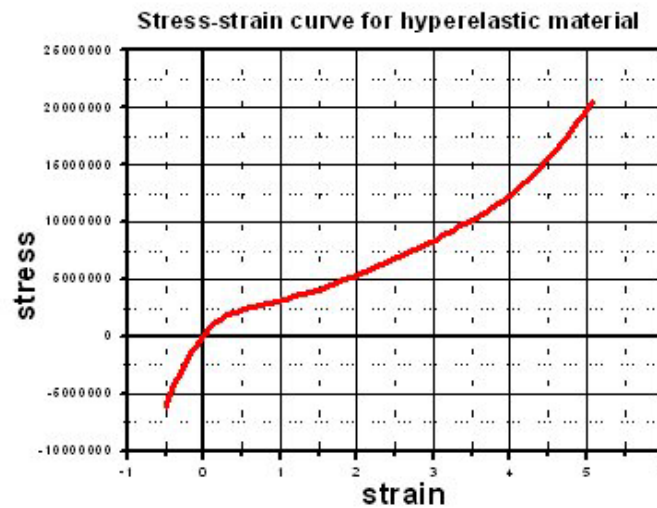


Figure 30 – Membrane

Experimental stress-strain curve is presented in Figure 31 - *Stress-strain curve*. Basing on experimental data obtained, Mooney-Rivlin's constants for determination of specific potential energy of 9-constant Mooney-Rivlin material were computed with use of ANSYS in-built procedures.

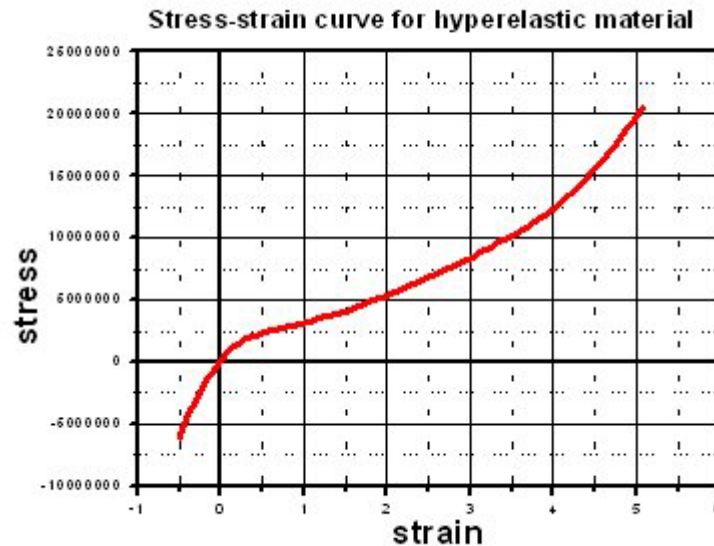


Figure 31 - Stress-strain curve

Figures 32, 33 - *FE model of multiplier 1*, *FE model of multiplier 2* demonstrate a 3D FE model of the multiplier containing 38690 SOLID92 elements. Figure 34 - *FE model of Membrane* represents a 3D FE model of the membrane. It contains 5963 HYPER158 elements. The following assumptions were taken for the procedure of the membrane structural analysis:

- 1) Owing to the symmetry of the construction and boundary conditions one half of the membrane is modeled;
- 2) The membrane is under action of uniformly disturbed pressure P ;
- 3) The inner surface of the membrane is constrained in all directions (modeling of "no-separation" contact interaction of the membrane and punch). This assumption may be substantiated by the fact that under high external pressure and presence of high coefficient of friction ($\mu > 1$), relative slipping of the membrane and the punch will take place only at the initial stage of loading, so this effect may be neglected.

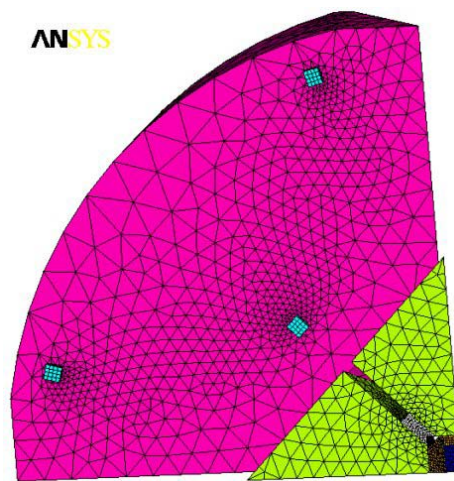


Figure 32 - FE model of multiplier 1

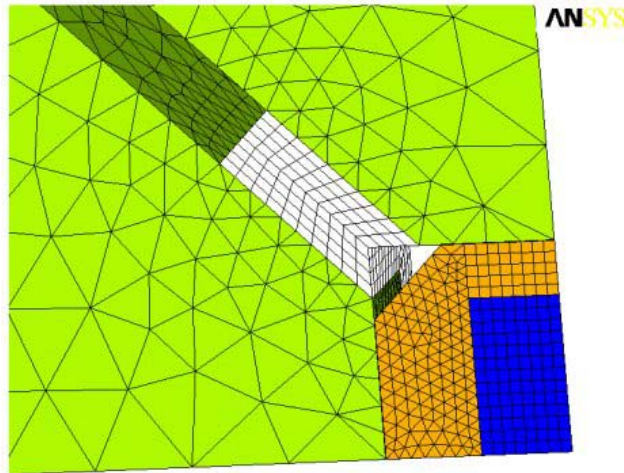


Figure 33 - FE model of multiplier 2

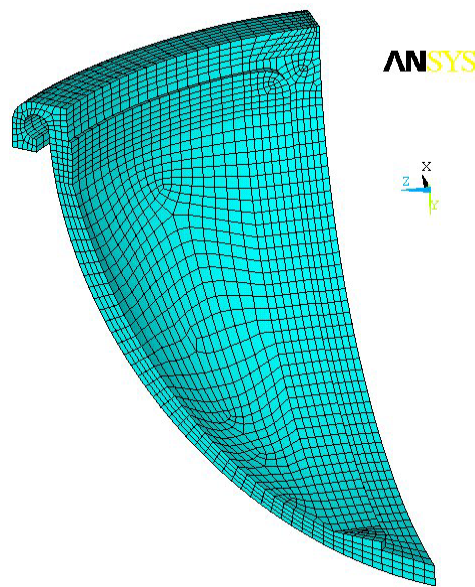


Figure 34 - FE model of membrane

Results

The analysis of the results obtained for the punch (see Figure - 35 *Equivalent stress in the punch*) shows that in the corners and edges of the contact triangular area the exceeding of yield stress for steel takes place. This gives evidence of existence of local plastic zones and necessity of using elasto-plastic model material model for more correct evaluation of the construction stressed state.

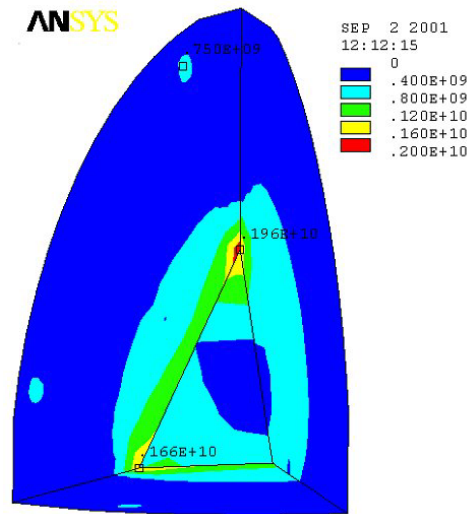


Figure 35 - Equivalent stress in the punch

Figures 36, 37 - *Equivalent stress in the capsule, Equivalent stress in the insert* present equivalent stress field for the capsule and hard-alloy inserts. The analysis of the results obtained shows that on the inner surface of the hard-alloy inserts and outer surface of the capsule there are stress concentration zones caused by linearly elastic behavior of materials. It may be supposed that on condition of taking into account elasto-plastic behavior of material, the decrease of stress concentration factor will take place. Solution of the problem with account of the elasto-plastic properties of the material is impended because of the absence of necessary data.

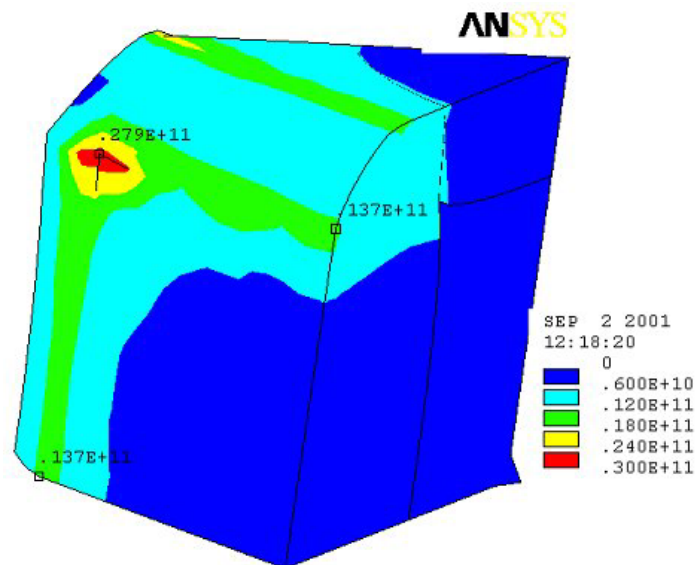


Figure 36 - Equivalent stress in the capsule

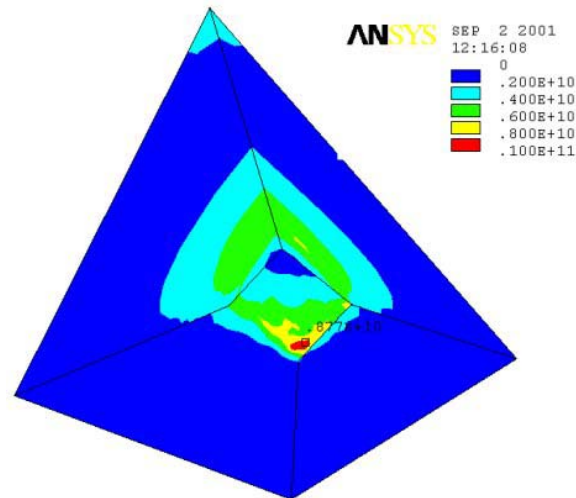


Figure 37 - Equivalent strain in the insert

Distribution of equivalent stress and strain intensity in the membrane is presented in Figures 38, 39 - *Equivalent stress in the membrane, Equivalent strain in the membrane*. As it may be see, two stress concentrators are observed in the upper area of the membrane - on the outer an the inner surfaces. Maximal value of strain intensity on the outer surface comes to 230 %, on the inner surface - to 320 %.

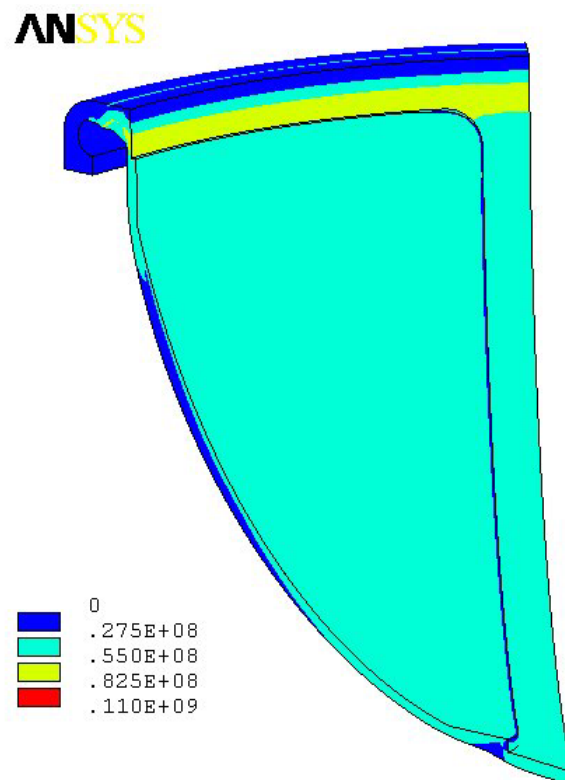


Figure 38 - Equivalent stress in the membrane

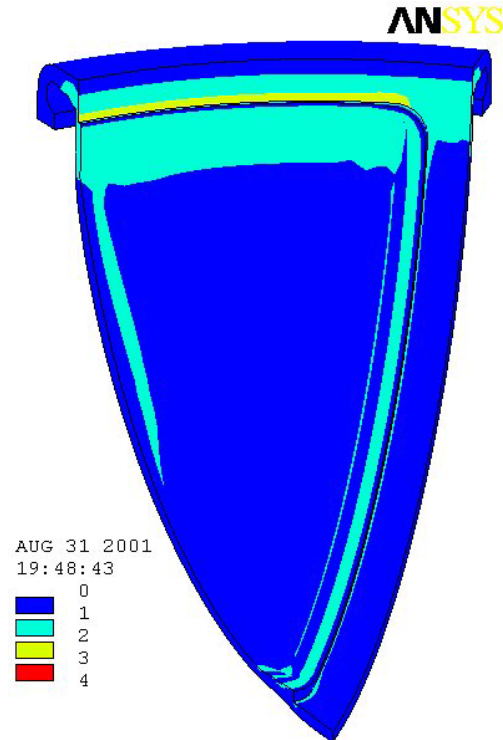


Figure 39 - Equivalent strain in the membrane

Conclusion

A structural analysis of the high-pressure vessel was implemented. The research performed allowed evaluation of strength of all parts of the vessel and optimization of the outline size aiming to decrease steel intensity. Experimental investigation carried out allowed us to come to the conclusion of adequacy of mathematical models chosen and validity of the results obtained by FE research.

This paper contains the results of researches implemented within a Bachelor Project.

Acknowledgments

The authors would thank Dr. Shtukin L.V. for providing with data of experimental research of strain fields in case body.

References

- 1) Ansys theory reference. Eleventh edition. SAS IP, Inc.
- 2) Gill, F., Murrey, U., and Right, M., 1985, "Applied optimization", Moscow, Mir. (In Russian).
- 3) Foye, R.L., "Non-elastic micro-mechanics of shrinkage stresses in composites", Mechanics, New aspects in international science, Issue 16, Non-elastic mechanical properties of composites, Ed. Ishlinsky, A.Yu., Cherny, G.K., pp. 249-294. (In Russian).
- 4) Hall Tracy H., 1961, "The synthesis of diamond", Journal of Chemical Education. Vol. 38, No 9, pp.1-7.
- 5) Ogden, R.W., 1997, "Non-linear elastic deformations", Mineola, NY, Dover Publ. Inc.
- 6) Sukharev, I.P., 1987, "Experimental methods for strain analysis", Moscow, Mashinostroenie. (In Russian).